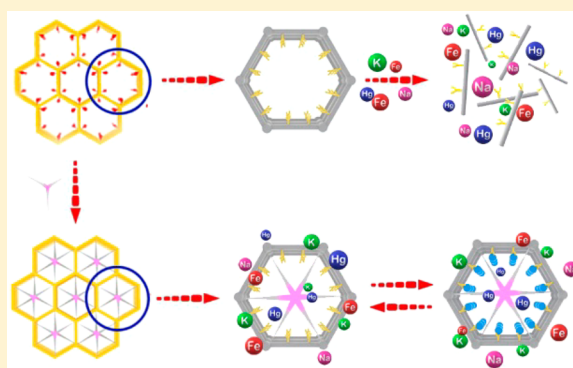


## Introduction of Molecular Building Blocks to Improve the Stability of Metal–Organic Frameworks for Efficient Mercury Removal

Shu-Yi Jiang,<sup>†,‡</sup> Wen-Wen He,<sup>§,‡</sup> Shun-Li Li,<sup>‡</sup> Zhong-Min Su,<sup>\*,†,§</sup> and Ya-Qian Lan<sup>\*,‡,§</sup><sup>†</sup>Institute of Functional Material Chemistry, Faculty of Chemistry, Northeast Normal University, Changchun, 130024 Jilin, China<sup>‡</sup>China Jiangsu Key Laboratory of Biofunctional Materials, School of Chemistry and Materials Science, Nanjing Normal University, Nanjing, 210023 Jiangsu, China<sup>§</sup>School of Chemistry and Life Science, Advanced Institute of Materials Science, Changchun University of Technology, Changchun 130012, China

## S Supporting Information

**ABSTRACT:** With expanding human needs, many heavy metals were mined, smelted, processed, and manufactured for commercialization, which caused serious environmental pollutions. Currently, many adsorption materials are applied in the field of adsorption of heavy metals. Among them, the principle of many mercury adsorbents is based on the interaction between mercury and sulfur. Here, a S-containing metal–organic framework NENU-400 was synthesized for effective mercury extraction. Unfortunately, the skeleton of NENU-400 collapsed easily when exposed to the mercury liquid solution. To improve the stability, a synthetic strategy installing molecular building blocks (MBBs) into the channels was used. Modified by the MBBs, a more stable nanoporous framework was synthesized, which not only exhibits a high capacity of saturation mercury uptake but also shows high selectivity and efficient recyclability.



## ■ INTRODUCTION

Mercury has been proven to be a toxic heavy metal which is harmful to our brains, livers, and central nervous systems.<sup>1</sup> Many methods such as amalgamation, chemical precipitation, magnetic separation, and ion exchange have been applied in the remediation of mercury heavy metal pollution, which are discharged by removing the mercury from industry products, byproducts, and production processes. But all the methods have the limitations of being nonreusable or having low uptake or slow sorption kinetics, which badly affect the application in daily practice.<sup>2–6</sup> Therefore, constructing reusable materials to satisfy the demands of capacity, efficiency, reusability, and selectivity is still a challenge to chemistry science.

With characteristics such as high porosities, large surface areas, and tunable pore surface properties, metal–organic frameworks (MOFs) have drawn considerable attention in significant prospects for promoting the energy and environmental sustainable development, including gas adsorption separation, catalysis, and proton conduction.<sup>7–17</sup> With the application as priority, functional oriented synthesis strategy presents a progressive evolution for the construction of MOF materials.<sup>18–20</sup> Because of the strong Hg–S interactions, MOFs with the introduction of free-standing sulfur groups have proved to be excellent solid-phase sorbents to effective mercury uptake.<sup>21,22</sup> This represents a potentially powerful strategy for the molecular design of MOFs; while the carboxyl groups bind

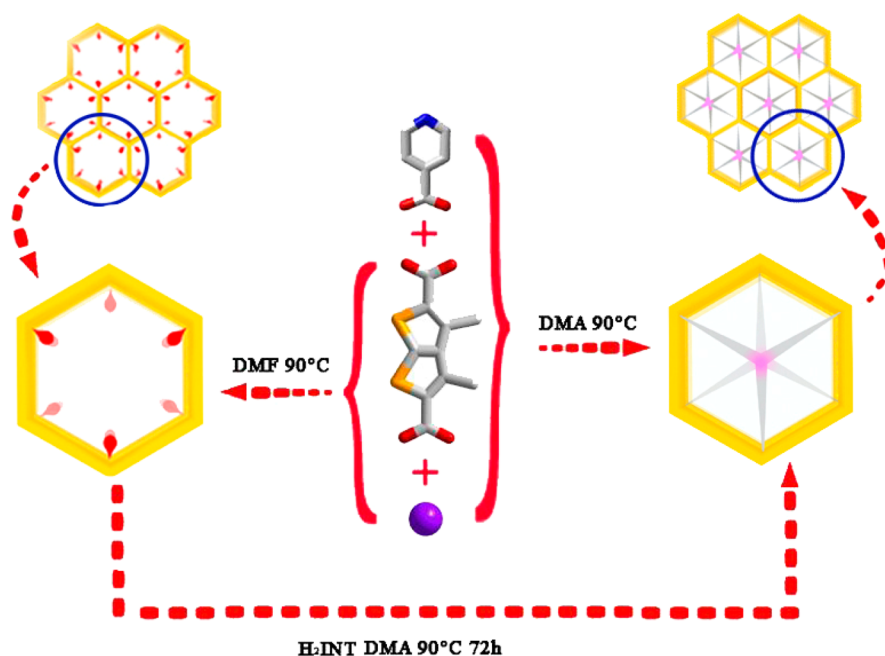
metal ions for network formation, the sulfur groups can remain as free-standing secondary donor groups. Xu et al. reported the Zr-DMBD with the hard carboxyl and soft thiol functioning as effective mercury sorption, and Dong et al. successfully synthesized thiol-derived Cr-MIL-101-AS by means of the postsynthetic modification method which shows excellent adsorbent ability in removing mercury ions from water.<sup>23,24</sup> To efficiently remove Hg(II), we designed and synthesized a suitable type of MOF NENU-400, which has free-standing thioether groups. The structure of NENU-400 is arranged as 6-connected *acs* (MIL-88B)<sup>25</sup> topology with the  $\text{Co}_3(\mu_3\text{-OH})(\text{RCOO})_6(\text{H}_2\text{O})_3$  clusters; the specific configurations of the open metal sites (OMSs) can fix various monodentate guest molecules to form a structurally decorated MOF. Unfortunately, the structure of NENU-400 easily collapsed during the process of mercury removal. To address this issue and also maintain its surface areas and functional sites, we incorporated predesigned molecular building blocks (MBBs) as the upholders into the pore channels of NENU-400 to get NENU-401 (see Scheme 1). With the MBBs, NENU-401 shows an exceptional saturated adsorption of mercury as  $\sim 600 \text{ mg g}^{-1}$  and effectively decreased Hg(II) concentration from 10 ppm to an extremely low level as 0.02 ppb. It also can efficiently

Received: March 15, 2018

Published: May 8, 2018



**Scheme 1.** Schematic Representation of the Interrelated Structures for NENU-400 and Reformed NENU-401 via the Introduction of Generated Size-Matching MBBs into the Open Channels



remove 99.7% mercury within a few minutes. Furthermore, NENU-401 is not only readily regenerated and recycled without significant loss of mercury adsorption capacity but also has high selectivity of mercury in solutions containing other background metal ions.

## EXPERIMENTAL SECTION

**Synthesis of NENU-400 and NENU-401.** Solvothermal reactions of  $\text{Co}(\text{NO}_3)_2 \cdot 6\text{H}_2\text{O}$  with  $\text{H}_2\text{DMTDC}$  yield pink crystals of NENU-400  $\{[\text{Co}_3(\mu_3\text{-OH})(\text{H}_2\text{O})_3(\text{DMTDC})_3](\text{NO}_3)_{10} \cdot (\text{H}_2\text{O})_6(\text{DMF})_6\}_n$  and purple crystals of NENU-401  $\{[\text{Co}_3(\mu_3\text{-OH})(\text{DMTDC})_3(\text{INT})_3] \cdot [\text{Co}_2(\text{OH})(\text{H}_2\text{O})_2](\text{NO}_3)_{19} \cdot (\text{H}_2\text{O})_7(\text{DMA})_{11}\}_m$  without or with the introduction of INT, respectively (DMTDC = 3,4-dimethylthieno[2,3-*b*]thiophene-2,5-dicarboxylic acid, INT = isonicotinate, DMF = *N,N*-dimethylformamide, and DMA = *N,N*-dimethylacetamide). Single crystal X-ray diffraction analysis reveals that NENU-400 crystallizes in the trigonal space group  $P\bar{3}1c$ . The structure consists of  $\text{Co}_3(\mu_3\text{-OH})$  cores and  $\text{DMTDC}^{2-}$  ligands (see Figure 1a), which is similar to the structure of MIL-88B. Every  $\text{Co}(\text{II})$  ion is six-coordinated with one  $\mu_3\text{-OH}^-$ , one coordinated water molecule, and four oxygen atoms from four different  $\text{DMTDC}^{2-}$  ligands.<sup>26</sup> Every five  $\text{Co}_3(\mu_3\text{-OH})$  cores and six  $\text{DMTDC}^{2-}$  ligands compose a trigonal bipyramid-type cage (see Figure 1c). From a topological viewpoint, the whole structure of NENU-400 can be classified as a 6-connected *acs* topological network. Also, this type of connection constructs a three-dimensional porous framework which has hexagonal honeycomb channels running along the *c* axis, with an aperture size of approximately 7.79 Å (see Figure 1e).

In the structure of NENU-400, each  $\text{Co}_3(\mu_3\text{-OH})$  core has three coordinated water molecules pointing to the center of the hexagonal channel and taking a  $C_3$  symmetry. To improve the stability of NENU-400, we try to put three-connected supports to replace these monodentate water molecules. Considering the geometric feature of the structure, we selected a tridentate MBB  $[\text{Co}_2(\text{INT})_3(\text{H}_2\text{O})_2]$  which not only fits in its planar tritopic with  $C_3$  symmetry but also matches the size and charge requirements of the channels. We added isonicotinic acid into NENU-400's reaction system and got a new crystal NENU-401. Single crystal X-ray diffraction analysis reveals that NENU-401 crystallizes in the same space group, which has cell parameters nearly identical to those of NENU-400. As we expected,

INT<sup>2-</sup> ligands have replaced the single coordinated water molecules successfully (see Figure 1b). MBBs  $[\text{Co}_2(\text{INT})_3(\text{H}_2\text{O})_2]$  are installed into the channels as three-connected supports which improved the stability of the frameworks. With the tridentate MBBs, NENU-401 is apparently more stable than NENU-400, which was shown by PXRD results (see Figures S7 and S8). NENU-401 not only can exist stable in air for one week at least, but also can be stable in some organic solvents. The thermal stabilities show that NENU-400 was stable up to  $\sim 140^\circ\text{C}$ , and then the structure decomposed. It also revealed that NENU-401 has thermal stability up to  $\sim 263^\circ\text{C}$ , and there is a  $\sim 123^\circ\text{C}$  improvement (see Figure S9). Meanwhile the trigonal bipyramid-type cage in NENU-400 has changed into a hexagonal dipyramidal form, but the size of the cage is maintained (see Figure 1c and 1d). With the insertion of three-connected supports into the *acs* net, a new framework type, *pacs* (partitioned *acs*) has generated.<sup>27</sup> Deeper analysis of the channels which have been divided into six small triangular ones shows that the diameter of the new channel is  $\sim 3.75$  Å (see Figure 1f).

**Material Characterization.** The thermal stabilities of NENU-400 and NENU-401 (see Figure S9) were tested by thermogravimetric analysis (TGA) under a dry  $\text{N}_2$  atmosphere. There was a continuous mass loss of 27.3% from 20 to  $142^\circ\text{C}$  (calcd 27.6%), corresponding to the reduce of  $\text{H}_2\text{O}$  and DMF molecules in NENU-400. The framework was stable up to  $\sim 140^\circ\text{C}$ , and then the structure decomposed. NENU-401 showed a continuous weight loss of 30.22% from 48 to  $263.1^\circ\text{C}$  (calcd 29.8%), it revealed that NENU-401 has thermal stability up to  $\sim 263^\circ\text{C}$  (see Figure S2).

**Powder X-ray Diffraction.** To investigate stability of these two compounds, the samples were exposed to air for one week. PXRD patterns before and after exposure demonstrate that NENU-400 decomposed, while NENU-401 could preserve its structural integrity. To exchange guest molecules in the frameworks and further evaluate their chemical stabilities, NENU-400 and NENU-401 were immersed in acetone and acetonitrile for 3 days. NENU-400 collapsed after being immersed, on the contrary, the measured PXRD pattern of NENU-401 is identical with its simulated PXRD pattern showing the framework is maintained (see Figures S7 and S8).

## RESULTS AND DISCUSSION

**Adsorption Performances of NENU-400 and NENU-401 for Mercury.** To assess the absorption capacity of  $\text{Hg}(\text{II})$ ,

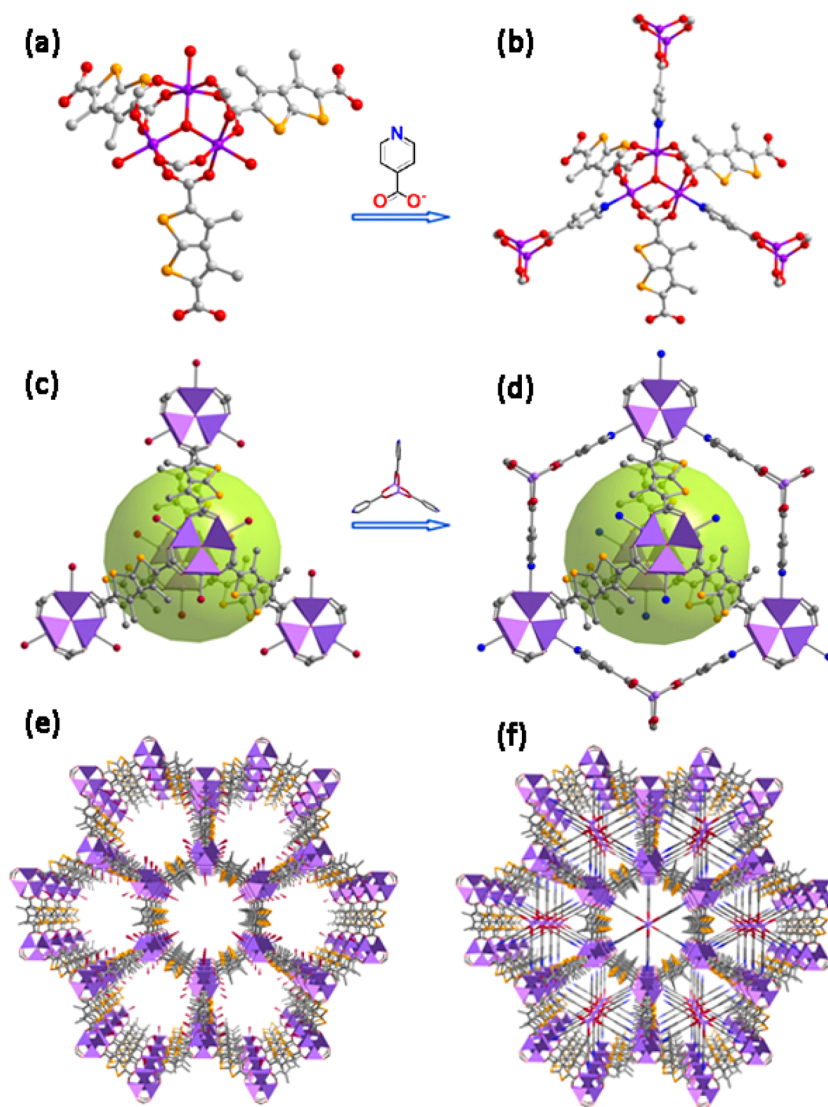


**Figure 1.** (a and b) The coordination environments of inorganic SBUs in NENU-400 and NENU-401, respectively. (c and d) Two types of cages in NENU-400 and NENU-401, respectively. (e and f) View of the 3D structures of NENU-400 and NENU-401 along the *c* axis, respectively. (Purple balls: Co; red balls: O; yellow balls: S; blue balls: N; gray balls: C).

NENU-400, and NENU-401 were exposed to Hg(II) solution with different concentration gradient ranging from 10 to 900 ppm. After 12 hours, the crystals were extracted from the solutions and the adsorption quantities of Hg(II) were analyzed by ICP-MS (Inductively Coupled Plasma Mass Spectrometry). As shown in Figure S10, there is almost no adsorption taking place in NENU-400. This phenomenon can be ascribed to the collapse of NENU-400 frameworks when exposed to the Hg(II) solution. By contrast, NENU-401 with trident bearings exhibits excellent adsorption behavior of Hg(II) (see Figure 2a). The equilibrium adsorption isotherm data fit the Langmuir model very well, yielding a correlation coefficient as high as 0.998. The maximum capacity of NENU-401 for mercury is  $596.57 \text{ mg g}^{-1}$ , which is higher than most thiol-functionalized MOFs and other kinds of reported materials (see Table S4.). The outstanding saturated Hg(II) removal capacity can be ascribed to high accessibility of thioether groups, which are dispersed uniformly on the channel surface of the highly porous NENU-401.

In addition to the high adsorbing capacity of Hg(II), NENU-401 is also prominent in the removal effectiveness. We

established a system with  $\text{Hg}(\text{NO}_3)_2$  (50 mL, 10 ppm) and NENU-401 (30 mg) at  $25^\circ\text{C}$  to investigate the reaction kinetics (Supporting Information). Surprisingly, it exhibited a considerable removal efficiency; over 99.7% of Hg(II) was adsorbed within 10 min at equilibrium (see Figure 2c). When the contact time was extended to 3 h, the Hg(II) concentration was decreased to 2 ppb. The adsorption rate constant ( $K_2$ , Supporting Information) fitting with the pseudo-second-order model was evaluated to be  $0.99 \text{ g mg}^{-1} \text{ min}^{-1}$  (see Figure 2d and e). Such high rate performance observed for NENU-401 can be attributed to the large amount of sulfur groups on the inner surface and well-defined pore channel size, which facilitate the diffusion of Hg(II) very well. Distribution coefficient ( $K_d$ , Supporting Information) is used to evaluate the affinity of sorbent for metal ions generally. The  $K_d$  value of NENU-401 at  $25^\circ\text{C}$  was calculated to be  $8.3 \times 10^6 \text{ mL g}^{-1}$ , which exhibits distinct superiority compared with other materials such as commercial resins ( $5.1 \times 10^5 \text{ mL g}^{-1}$ ), sulfide-modified mesoporous carbons ( $6.82 \times 10^5 \text{ mL g}^{-1}$ ), and LHMS-1 ( $6.4 \times 10^6 \text{ mL g}^{-1}$ ).<sup>28–30</sup>



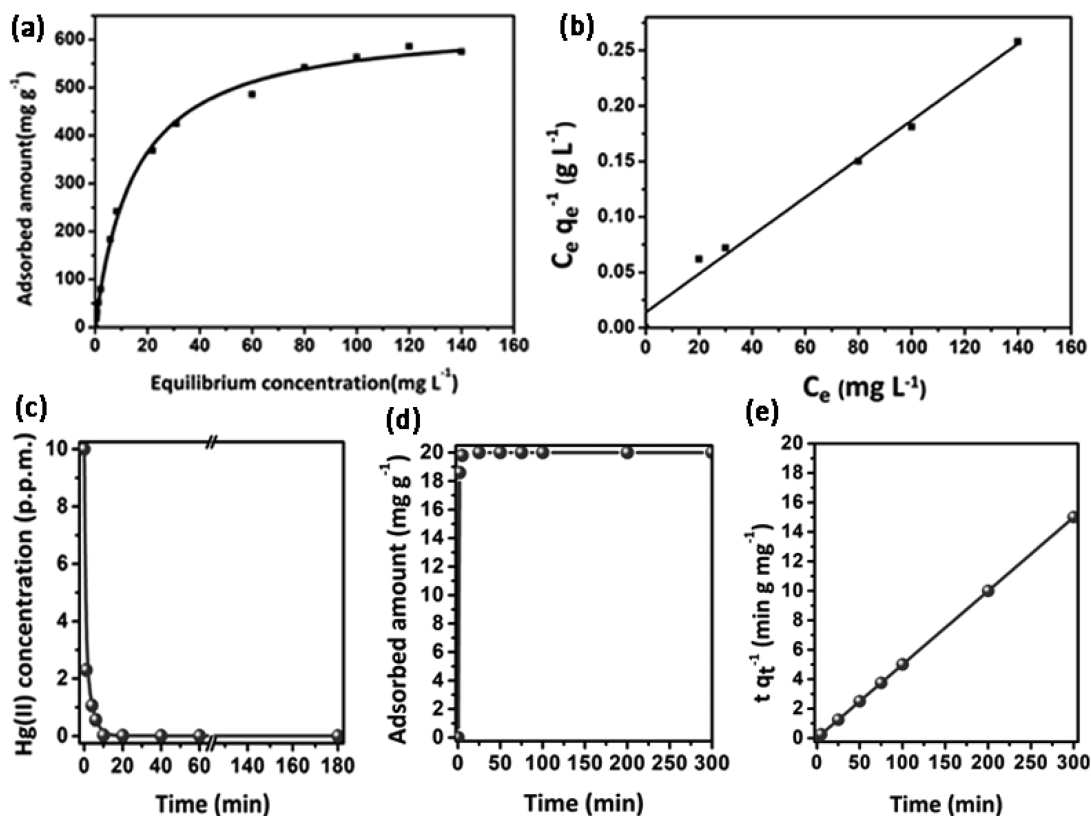


**Figure 2.** (a) Hg(II) adsorption isotherm of NENU-401 after 12 h. (b) The linear regression of the adsorption isotherm by fitting the equilibrium adsorption data with Langmuir adsorption model. (c) Hg(II) sorption kinetics of NENU-401 under the initial Hg(II) concentration of 10 ppm. (d) Adsorption curve of NENU-401 Hg(II) versus contact time in solution. (e) Pseudo-second-order kinetic plot of NENU-401 for the adsorption at Hg(II) concentration of 10 ppm.

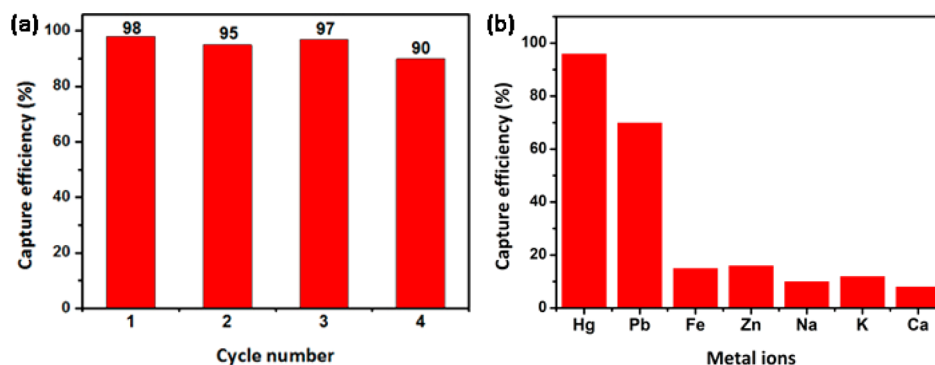


**Figure 3.** (a) Cycle performance for Hg(II) removal. (b) Capture efficiency in removing metal ions.

Regeneration and recycling property are two important standards to evaluate an adsorption material for practical application. Considering the strong interaction between the framework and Hg(II) ions, thioglycol was chosen as an eluent. Hg(II)-captured NENU-401 was demetallized by rinsing with thioglycol solution, and the regenerated NENU-401 was employed for adsorption again. After 4 cycles, ICP-MS reveals that the crystal of NENU-401 can still retain 90% of the original capacity (see Figure 3a). In addition, powder XRD analyses demonstrate that NENU-401 can retain high crystallinity after every cycle (see Figure S11). Because of the thioether donors in NENU-401, there is a considerable advantage in cyclicity over other materials with thiol groups such as SH@SiO<sub>2</sub>, JUC-62, Fe<sub>3</sub>O<sub>4</sub>-R6G, and so on.<sup>31–33</sup> Selectivity is another crucial factor for practical use of materials. NENU-401 was steeped into the

mixture solution of K(I), Na(II), Hg(II), Pb(II), Zn(II), Ca(II), Mg(II), and Fe(III) ions at each concentration of 10 ppm. As depicted in Figure 3b, NENU-401 could remove Hg(II) and Pb(II) effectively, but scarcely capture the rest of the metal ions such as K(I), Na(II), Zn(II), Ca(II), Mg(II), and Fe(III).

To study the efficient mercury removal performance in NENU-401, we utilized XPS and FT-IR to monitor this adsorption progress. XPS signals indicated that the appearance of Hg(II) at 102 and 106 eV assigned to the Hg 4f<sub>7/2</sub> and Hg 4f<sub>5/2</sub> orbital, respectively, in the crystal of NENU-401-Hg. The S 2p XPS spectra showed a 1 eV shift in NENU-401-Hg comparing to that of NENU-401, which demonstrated the strong binding interactions between the Hg(II) and S species (see Figure S12). Furthermore, the lack of characteristic S–H

stretching mode at  $2515\text{ cm}^{-1}$  in the IR spectrum of NENU-401-Hg could meanwhile verify the interactions between mercury and sulfur species (see Figure S13).<sup>34</sup>

## CONCLUSION

In conclusion, by choosing the appropriate carboxylate ligands with free-standing thioether groups, the functional MOF NENU-400 was synthesized. Considering the characteristics in the frameworks, we synthesized a more rigid skeleton MOF by introducing MBBs into the channels. The synthetic strategy is the first example to improve the rigid of skeletons for making it capable of efficient mercury adsorption. Significantly, the modified stable frameworks have shown remarkable mercury adsorption ability which the capacity of the activated crystals is close to  $600\text{ mg g}^{-1}$ . Also, the  $K_2$  is  $0.99\text{ g mg}^{-1}\text{ min}^{-1}$ , and the  $K_d$  of NENU-401 at  $25\text{ }^\circ\text{C}$  is calculated to be  $8.3 \times 10^6\text{ mL g}^{-1}$ , which show evident preponderance comparing to other MOFs. Furthermore, this capacity of NENU-401 can retain 90% of the original state after 4 cycles. All the results prove that NENU-401 has the potential to be applied in industrial processes. The synthetic strategy presents a progressive evolution for the construction of S-containing frameworks, and the development of MOF materials for adsorption of mercury is currently underway.

## ASSOCIATED CONTENT

### Supporting Information

The Supporting Information is available free of charge on the ACS Publications website at DOI: [10.1021/acs.inorgchem.8b00704](https://doi.org/10.1021/acs.inorgchem.8b00704).

Ligand synthesis, crystal data, general procedures for Hg(II) adsorption, PXRD patterns, TGA curves, XPS spectra, and IR spectra (PDF)

### Accession Codes

CCDC 1584139–1584140 contain the supplementary crystallographic data for this paper. These data can be obtained free of charge via [www.ccdc.cam.ac.uk/data\\_request/cif](http://www.ccdc.cam.ac.uk/data_request/cif), by emailing [data\\_request@ccdc.cam.ac.uk](mailto:data_request@ccdc.cam.ac.uk), or by contacting The Cambridge Crystallographic Data Centre, 12 Union Road, Cambridge CB2 1EZ, UK; fax: +44 1223 336033.

## AUTHOR INFORMATION

### Corresponding Authors

\*E-mail: [yqlan@nenu.edu.cn](mailto:yqlan@nenu.edu.cn).

\*E-mail: [zmsu@nenu.edu.cn](mailto:zmsu@nenu.edu.cn).

### ORCID

Zhong-Min Su: 0000-0002-3342-1966

Ya-Qian Lan: 0000-0002-2140-7980

### Author Contributions

<sup>†</sup>S.-Y.J. and W.-W.H. contributed equally.

### Notes

The authors declare no competing financial interest.

## ACKNOWLEDGMENTS

This work was financially supported by the National Natural Science Foundation of China (Grants 21622104, 21471080, and 21701016), the Education Department of Jilin Province (Grant JJKH20181020KJ), the Science and Technology Development Planning of Jilin Province (Grant 20160520124JH), the Priority Academic Program Development of Jiangsu Higher Education Institutions, and the

Foundation of Jiangsu Collaborative Innovation Center of Biomedical Functional Materials.

## REFERENCES

- (1) McNutt, M. Mercury and Health. *Science* **2013**, *341*, 1430.
- (2) Mandel, K.; Hutter, F.; Gellermann, C.; SEXTL, G. Modified Superparamagnetic Nanocomposite Microparticles for Highly Selective Hg-II or Cu-II Separation and Recovery from Aqueous Solutions. *ACS Appl. Mater. Interfaces* **2012**, *4*, 5633–5642.
- (3) Tadjarodi, A.; Abbaszadeh, A. A magnetic nanocomposite prepared from chelator-modified magnetite ( $\text{Fe}_3\text{O}_4$ ) and HKUST-1 (MOF-199) for separation and preconcentration of mercury(II). *Microchim. Acta* **2016**, *183*, 1391–1399.
- (4) Qu, Z.; Yan, L.; Li, L.; Xu, J.; Liu, M.; Li, Z.; Yan, N. Ultraeffective ZnS Nanocrystals Sorbent for Mercury(II) Removal Based on Size-Dependent Cation Exchange. *ACS Appl. Mater. Interfaces* **2014**, *6*, 18026–18032.
- (5) Cui, L. M.; Guo, X. Y.; Wei, Q.; Wang, Y. G.; Gao, L.; Yan, L. G.; Yan, T.; Du, B. Removal of mercury and methylene blue from aqueous solution by xanthate functionalized magnetic graphene oxide: Sorption kinetic and uptake mechanism. *J. Colloid Interface Sci.* **2015**, *439*, 112–120.
- (6) Li, K.; Wang, Y. W.; Huang, M.; Yan, H.; Yang, H.; Xiao, S. J.; Li, A. M. Preparation of chitosan-graft-polyacrylamide magnetic composite microspheres for enhanced selective removal of mercury ions from water. *J. Colloid Interface Sci.* **2015**, *455*, 261–270.
- (7) Furukawa, H.; Cordova, K. E.; O’Keeffe, M.; Yaghi, O. M. The chemistry and applications of metal-organic frameworks. *Science* **2013**, *341*, 1230444.
- (8) Rodenas, T.; Luz, I.; Prieto, G.; Seoane, B.; Miro, H.; Corma, A.; Kapteijn, F.; Llabrés i Xamena, F. X.; Gascon, J. Metal-organic framework nanosheets in polymer composite materials for gas separation. *Nat. Mater.* **2015**, *14*, 48–55.
- (9) Xue, D. X.; Belmabkhout, Y.; Shekhan, O.; Jiang, H.; Adil, K.; Cairns, A. J.; Eddaoudi, M. Tunable Rare Earth fcu-MOF Platform: Access to Adsorption Kinetics Driven Gas/Vapor Separations via Pore Size Contraction. *J. Am. Chem. Soc.* **2015**, *137*, 5034–5040.
- (10) Chughtai, A. H.; Ahmad, N.; Younus, H. A.; Laypkov, A.; Verpoort, F. Metal-organic frameworks: versatile heterogeneous catalysts for efficient catalytic organic transformations. *Chem. Soc. Rev.* **2015**, *44*, 6804–6849.
- (11) Zhang, F. M.; Dong, L. Z.; Qin, J. S.; Guan, W.; Liu, J.; Li, S. L.; Lu, M.; Lan, Y. Q.; Su, Z. M.; Zhou, H. C. Effect of Imidazole Arrangements on Proton-Conductivity in Metal-Organic Frameworks. *J. Am. Chem. Soc.* **2017**, *139*, 6183–6189.
- (12) Rogge, S. M. J.; Bavykina, A.; Hajek, J.; Garcia, H.; Olivares-Suarez, A. I.; Sepúlveda-Escribano, A.; Vimont, A.; Clet, G.; Bazin, P.; Kapteijn, F.; Daturi, M.; Ramos-Fernandez, E. V.; Llabrés i Xamena, F. X.; Van Speybroeck, V.; Gascon, J. Metal-organic and covalent organic frameworks as single-site catalysts. *Chem. Soc. Rev.* **2017**, *46*, 3134.
- (13) Adil, K.; Belmabkhout, Y.; Pillai, R. S.; Cadiau, A.; Bhatt, P. M.; Assen, A. H.; Maurin, G.; Eddaoudi, M. Gas/vapour separation using ultra-microporous metal-organic frameworks: insights into the structure/separation relationship. *Chem. Soc. Rev.* **2017**, *46*, 3402.
- (14) Hu, M.; Reboul, J.; Furukawa, S.; Radhakrishnan, L.; Zhang, Y. J.; Srinivasu, P.; Iwai, H.; Wang, H. J.; Nemoto, Y.; Suzuki, N.; Kitagawa, S.; Yamauchi, Y. Direct synthesis of nanoporous carbon nitride fibers using Al-based porous coordination polymers (Al-PCPs). *Chem. Commun.* **2011**, *47*, 8124–8126.
- (15) Radhakrishnan, L.; Reboul, J.; Furukawa, S.; Srinivasu, P.; Kitagawa, S.; Yamauchi, Y. Preparation of microporous carbon fibers through carbonization of Al-based porous coordination polymer (Al-PCP) with furfuryl alcohol. *Chem. Mater.* **2011**, *23*, 1225–1231.
- (16) Chaikittisilp, W.; Torad, N. L.; Li, C. L.; Imura, M.; Suzuki, N.; Ishihara, S.; Ariga, K.; Yamauchi, Y. Synthesis of nanoporous carbon-cobalt-oxide hybrid electrocatalysts by thermal conversion of metal-organic frameworks. *Chem. - Eur. J.* **2014**, *20*, 4217–4221.

- (17) Zhang, W.; Jiang, X. F.; Zhao, Y. Y.; Carné-Sánchez, A.; Malgras, V.; Kim, J.; Kim, J. H.; Wang, S. B.; Liu, J.; Jiang, J. S.; Yamauchi, Y.; Hu, M. Hollow carbon nanobubbles: monocrystalline MOF nanobubbles and their pyrolysis. *Chem. Sci.* **2017**, *8*, 3538–3546.
- (18) Huang, R. W.; Wei, Y. S.; Dong, X. Y.; Wu, X. H.; Du, C. X.; Zang, S. Q.; Mak, T. C. W. Hypersensitive dual-function luminescence switching of a silver-chalcogenolate cluster-based metal-organic framework. *Nat. Chem.* **2017**, *9*, 689–697.
- (19) Wang, R.; Dong, X. Y.; Du, J.; Zhao, J. Y.; Zang, S. Q. MOF-derived bifunctional Cu<sub>3</sub>P nanoparticles coated by a N,P-codoped carbon shell for hydrogen evolution and oxygen reduction. *Adv. Mater.* **2018**, *140*, 2363–2372.
- (20) Yuan, S.; Qin, J. S.; Xu, H. Q.; Su, J.; Rossi, D.; Chen, Y. P.; Zhang, L. L.; Lollar, C.; Wang, Q.; Jiang, H. L.; Son, D. H.; Xu, H. Y.; Huang, Z. H.; Zou, X. D.; Zhou, H.-C.; Zhou, H. C. [Ti<sub>8</sub>Zr<sub>2</sub>O<sub>12</sub>(COO)<sub>16</sub>] cluster: an ideal inorganic building unit for photoactive metal-organic frameworks. *ACS Cent. Sci.* **2018**, *4*, 105–111.
- (21) Abney, C. W.; Gilhula, J. C.; Lu, K.; Lin, W. Metal-organic framework templated inorganic sorbents for rapid and efficient extraction of heavy metals. *Adv. Mater.* **2014**, *26*, 7993–7997.
- (22) He, J.; Yee, K. K.; Xu, Z. T.; Zeller, M.; Hunter, A. D.; Chui, S. S. Y.; Che, C. M. Thioether side chains improve the stability, fluorescence, and metal uptake of a metal-organic framework. *Chem. Mater.* **2011**, *23*, 2940–2947.
- (23) Yee, K. K.; Reimer, N.; Liu, J.; Cheng, S. Y.; Yiu, S. M.; Weber, J.; Stock, N.; Xu, Z. Effective mercury sorption by thiol-laced metal-organic frameworks: in strong acid and the vapor phase. *J. Am. Chem. Soc.* **2013**, *135*, 7795–7798.
- (24) Liu, T.; Che, J. X.; Hu, Y. Z.; Dong, X. W.; Liu, X. Y.; Che, C. M. Alkenyl/thiol-derived metal-organic frameworks (MOFs) by means of postsynthetic modification for effective mercury adsorption. *Chem. - Eur. J.* **2014**, *20*, 14090–14095.
- (25) Wei, Y. S.; Zhang, M.; Liao, P. Q.; Lin, R. B.; Li, T. Y.; Shao, G.; Zhang, J. P.; Chen, X. M. Coordination templated [2 + 2+2] cyclotrimerization in a porous coordination framework. *Nat. Commun.* **2015**, *6*, 8348.
- (26) Thorp, H. H. Bond valence sum analysis of metal-ligand bond lengths in metalloenzymes and model complexes. *Inorg. Chem.* **1992**, *31*, 1585–1588.
- (27) Lu, X. F.; Liao, P. Q.; Wang, J. W.; Wu, J. X.; Chen, X. W.; He, C. T.; Zhang, J. P.; Li, G. R.; Chen, X. M. An alkaline-stable, metal hydroxide mimicking metal-organic framework for efficient electrocatalytic oxygen evolution. *J. Am. Chem. Soc.* **2016**, *138*, 8336–8339.
- (28) Shin, Y.; Fryxell, G. E.; Um, W.; Parker, K.; Mattigod, S. V.; Skaggs, R. Sulfur-functionalized mesoporous carbon. *Adv. Funct. Mater.* **2007**, *17*, 2897–2901.
- (29) Manos, M. J.; Petkov, V. G.; Kanatzidis, M. G. H<sub>2</sub>xMnxSn<sub>3</sub>-xS<sub>6</sub> (x = 0.11–0.25): A novel reusable sorbent for highly specific mercury capture under extreme pH conditions. *Adv. Funct. Mater.* **2009**, *19*, 1087–1092.
- (30) Yantasee, W.; Warner, C. L.; Sangvanich, T.; Addleman, R. S.; Carter, T. G.; Wiacek, R. J.; Fryxell, G. E.; Timchalk, C.; Warner, M. G. Removal of heavy metals from aqueous systems with thiol functionalized superparamagnetic nanoparticles. *Environ. Sci. Technol.* **2007**, *41*, 5114–5119.
- (31) Sohrabi, M. R. Preconcentration of mercury(II) using a thiol-functionalized metal-organic framework nanocomposite as a sorbent. *Microchim. Acta* **2014**, *181*, 435–444.
- (32) Wu, Y. Z.; Xu, G. H.; Wei, F. D.; Song, Q.; Tang, T.; Wang, X.; Hu, Q. Determination of Hg (II) in tea and mushroom samples based on metal-organic frameworks as solid phase extraction sorbents. *Microporous Mesoporous Mater.* **2016**, *235*, 204–210.
- (33) Wang, Z.; Wu, D.; Wu, G.; Yang, N.; Wu, A. Modifying Fe<sub>3</sub>O<sub>4</sub> microspheres with rhodamine hydrazide for selective detection and removal of Hg<sup>2+</sup> ion in water. *J. Hazard. Mater.* **2013**, *244*, 621–627.
- (34) Hoffmann, G. G.; Brockner, W.; Steinfatt, I. Bis(*n*-alkanethiolato) mercury(II) compounds, Hg(SC<sub>n</sub>H<sub>2n+1</sub>)<sub>2</sub> (*n* = 1 to 10, 12): preparation methods, vibrational spectra, GC/MS investigations, and exchange reactions with diorganyl disulfides. *Inorg. Chem.* **2001**, *40*, 977–985.